DIFFRACTIVE STRUCTURE FUNCTIONS AND QCD FITS*

S. LEVONIAN
DESY,
Notkestrasse 85,
22607 Hamburg, Germany
E-mail: levonian@mail.desy.de

A recent progress is reviewed in our understanding of inclusive diffraction in deeply inelastic regime at HERA. New precision measurements are now available from both H1 and ZEUS collaborations. A new set of diffractive parton distribution functions, determined from the H1 data, is presented. It could be used to test factorization properties of diffractive scattering in different reactions.

1. Introduction

A significant progress has been achieved over the last decade in understanding the nature of *diffractive phenomena* at high energies. This is to a large extent due to the electron-proton collider HERA, which is an ideal place to study hard diffraction in deep-inelastic scattering (DIS). Already the term 'deep-inelastic diffraction' itself sounds as a paradox and goes against our intuition, based upon the experience of hadronic interactions in which diffraction was known to be predominantly soft peripheral process. HERA for the first time offers the possibility for the partonic structure of colour singlet exchange to be probed.

At the hadronic level diffraction is best described in the framework of Regge formalism[1,2] as a t-channel exchange of a leading trajectory with the vacuum quantum numbers, named *Pomeron*. Specific interest to diffraction as a 'physics of Pomeron' is related to the fact that the Pomeron exchange asymptotically dominates over all other contributions to the scattering amplitude, and thus represents the essence of strong interactions in high energy limit. Translating to the modern partonic language this reveals that colourless exchange is important in low-x regime (which is high energy limit of

*contribution to the conference proceedings "new trends in hera physics", ringberg castle, tegernsee, germany, 28 september - 3 october, 2003

QCD) where gluons expect to dominate. Since the diffractive cross section, being proportional to the gluon density squared, rises with energy faster than the total cross section unitarity correction effects, e.g. in a form of gluon saturation, are expected to be first seen in diffraction. Hence an interesting question is: can this be observed already at HERA?

Another aspect in which diffraction may play a key rôle is an interplay between soft and hard processes. Since both short distance and long distance physics contribute to diffractive DIS, HERA has high potential to provide new insight into non-perturbative QCD phenomena, as well as to bridge soft (Regge) and hard (pQCD) domains.

1.1. *Kinematics of Diffractive DIS at HERA*

Figure 1 sketches the generic diffractive process in electron-proton scattering. In addition to the usual DIS kinematic variables: photon virtuality, $Q^2 = -q^2$, Bjorken-x, $x = -q^2/2P \cdot q$ and inelasticity $y = Q^2/sx$ this process is characterized by the 4-momentum squared transferred at the proton vertex, $t = (P - p_Y)^2$ and the longitudinal momentum fraction of the colour singlet exchange relative to the incoming proton, $x_{I\!P} = q \cdot (P - p_Y)/q \cdot P$. Here P and q are 4-momenta of the interacting proton and photon respectively and s is ep centre of mass energy squared. Ratio of Bjorken-x to $x_{I\!P}$ defines another diffractive variable, $\beta = x/x_{I\!P}$, which can be interpreted as the longitudinal momentum fraction of the exchange that is carried by the struck quark.

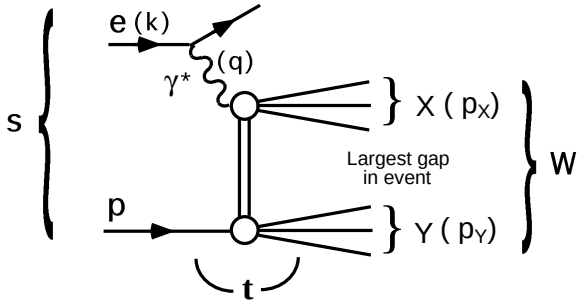

Figure 1. The generic diffractive process $ep \to eXY$ at HERA, in which interaction is mediated by colour singlet exchange between photon and proton vertecies, leading to the large rapidity interval separating final state systems X and Y.

After integrating over M_Y, which is not well measured at HERA, a four-

differential diffractive *reduced cross section*, $\sigma_r^{D(4)}$, can be defined through

$$\frac{d^4\sigma^D}{dx_{I\!P}\ dt\ d\beta\ dQ^2} = \frac{4\pi\alpha^2}{\beta Q^4}\left(1 - y + \frac{y^2}{2}\right)\sigma_r^{D(4)}(x_{I\!P}, t, \beta, Q^2), \qquad (1)$$

which is related to the diffractive structure functions F_2^D and F_L^D by

$$\sigma_r^D = F_2^D - \frac{y^2}{1+(1-y)^2}F_L^D. \qquad (2)$$

To a very good approximation $\sigma_r^D = F_2^D$ everywhere except possibly highest values of y. Furthermore, if the outgoing proton is not detected, the measurements are integrated over t: $\sigma_r^{D(3)} = \int \sigma_r^{D(4)} dt$.

1.2. *Understanding Diffraction in DIS*

The variety of the phenomenological models for diffractive DIS can be classified into three main categories.

1. Regge motivated models with factorizable Pomeron[3]. Internal partonic structure of such an object can be resolved in DIS. Regge factorization means that diffractive cross section can be factorized into Pomeron flux and its structure function. More generally, sub-leading reggeon contributions which are essential at high values of $x_{I\!P}$, should also be taken into account:

$$F_2^{D(4)}(x_{I\!P}, t, \beta, Q^2) = f_{I\!P}(x_{I\!P}, t)F_2^{I\!P}(\beta, Q^2) + f_{I\!R}(x_{I\!P}, t)F_2^{I\!R}(\beta, Q^2) \qquad (3)$$

with flux factors defined as

$$f_i(x_{I\!P}, t) = x_{I\!P}^{1-2\alpha_i(t)}e^{bt}, \qquad (4)$$

where $\alpha_i(t) = \alpha_i(0) + \alpha_i' t$ $(i = I\!P, I\!R)$ are Pomeron and reggeon trajectories respectively with intercept $\alpha_i(0)$ and slope α_i'.

2. Non-Pomeron mechanisms generating large rapidity gap events. For example, in soft colour interaction model[4] diffraction occurs through the normal boson-gluon fusion with additional emission of soft gluons, neutralizing the colour flow. As a consequence the model predicts leading gluon behaviour in which one gluon takes most of the momentum of the colour singlet exchange.

3. Colour dipole approach[5] to DIS in which interaction is viewed in the proton rest frame. This is especially convenient at low x, in which case virtual photon choose a specific Fock state to fluctuate into long before arriving to the proton target ($c\tau \approx 1/xM_p \simeq 1000$ fm at HERA). Hence the resulting cross section can be represented as a simple convolution of the photon wave function $|\gamma\rangle = \alpha_1|q\bar{q}\rangle + \alpha_2|q\bar{q}g\rangle + ...$ with colour dipole cross

section ($\sigma_{(q\bar{q})p}$, or $\sigma_{(q\bar{q}g)p}$). The models of this class[6] differ in the way they parameterise dipole cross sections. Their common strong feature is related to the fact, that once fitted to the inclusive DIS data, the same dipole cross sections with only one additional free parameter, related to t-dependence, should also describe diffractive phenomena in DIS.

Alternatively, one can employ a model independent approach using the concept of *diffractive parton distributions,* f_i^D. It is based on the rigorous proof[7] that QCD hard scattering factorization is valid for diffractive DIS, and hence the diffractive cross section (1) at fixed values $x_{I\!P}$ and t can be expressed as a convolution of universal partonic cross sections $\hat{\sigma}^{\gamma^* i}$ with f_i^D:

$$\sigma_r^D(4) \propto \sum_i \hat{\sigma}^{\gamma^* i}(x, Q^2) \otimes f_i^D(x, Q^2; x_{I\!P}, t). \tag{5}$$

The partonic cross section $\hat{\sigma}^{\gamma^* i}$ are the same as in inclusive DIS, and f_i^D, which are not known from first principles, should obey the DGLAP evolution equations. Hence the standard framework of NLO QCD can be applied to diffractive DIS in a similar manner as to inclusive DIS.

2. Experimental Techniques and data Samples

Several experimental techniques are used to measure diffractive processes at HERA. They have different advantages and drawbacks and are complementary to each other.

Most clean way is to detect scattered proton in the forward direction using so called *Roman pot* technique – remote detectors inserted in the beam pipe which together with machine magnets form a proton spectrometer. Such a method was exploited by both H1 and ZEUS experiments. It provides diffractive sample free of proton dissociative admixture and in addition enables t measurement, which in other methods is not directly measured and has to be integrated over. The method however suffers from low statistics, due to limited acceptance and the dependence on the beam conditions, which do not allow full luminosity to be collected.

To obtain high statistics sample one can use characteristic properties of the hadronic final state, as shown in Fig. 1. H1 and ZEUS follow slightly different approaches trying to to fully utilize their detector capabilities.

H1 method is based on the requirement of the large rapidity gap separating the leading baryon system Y from the photon dissociation system X. The rapidity gap is positively identified by the absence of activity in

pseudorapidity interval $3.2 < \eta < 7.5$, covered by various detector components. In this approach non-diffractive background is small and can be estimated using Monte Carlo simulation.

The extraction of the diffractive contribution in ZEUS is performed using so called M_X method, which is based on the fact that diffractive and non-diffractive final states have very different $\ln M_X^2$ distributions. The non-diffractive contribution exhibiting exponential fall-off towards lower M_X values is extrapolated underneath the diffractive plateau and statistically subtracted from the total M_X distribution. New Forward Plug Calorimeter[8], covering the pseudorapidity range $4 < \eta < 5$, was installed in 1998 and significantly improved capability of ZEUS detector for diffractive physics, by increasing the accessible M_X range by a factor of 1.7.

In the latter two methods selected diffractive samples are dominated by the single dissociative process $ep \to eXp$ with small admixture of double dissociation in which low mass proton dissociation system M_Y escapes in the beam hole undetected. Hence the measured cross sections are corrected to the region $M_Y < 1.6$ GeV and $|t| < 1$ GeV^2 in case of H1 and to $M_Y < 2.3$ GeV in case of ZEUS.

Both collaborations have released recently several new measurements with 2- to 5-fold increase in statistics and significant extension in the covered phase space as compared to the previously published data[9].

New measurement of the diffractive reduced cross section in the range $1.5 < Q^2 < 120$ GeV^2 by H1 collaboration is presented in Fig. 2. Two data samples[10,11] based on rapidity gap technique are in a good agreement with each other and with third measurement[12], covering $2 < Q^2 < 50$ GeV^2 and in which leading proton is detected in the forward spectrometer.

Inclusive diffractive cross section as measured by ZEUS collaboration[13] is shown in Fig. 3. With the exception of the lowest M_X bin a strong rise with energy, W, is observed. The data[14] in the transition region between DIS and quasi-real photon-proton interactions (see Fig. 4) exhibit a behaviour very similar to that of the total photon-proton cross section[15]. Namely, the diffractive cross section falls rapidly with Q^2 at high virtualities, while at $Q^2 \to 0$ the cross section dependence on Q^2 flattens off. This behaviour is broadly described by the colour dipole model[16] in which virtual photon fluctuates into $q\bar{q}$ and $q\bar{q}g$ states.

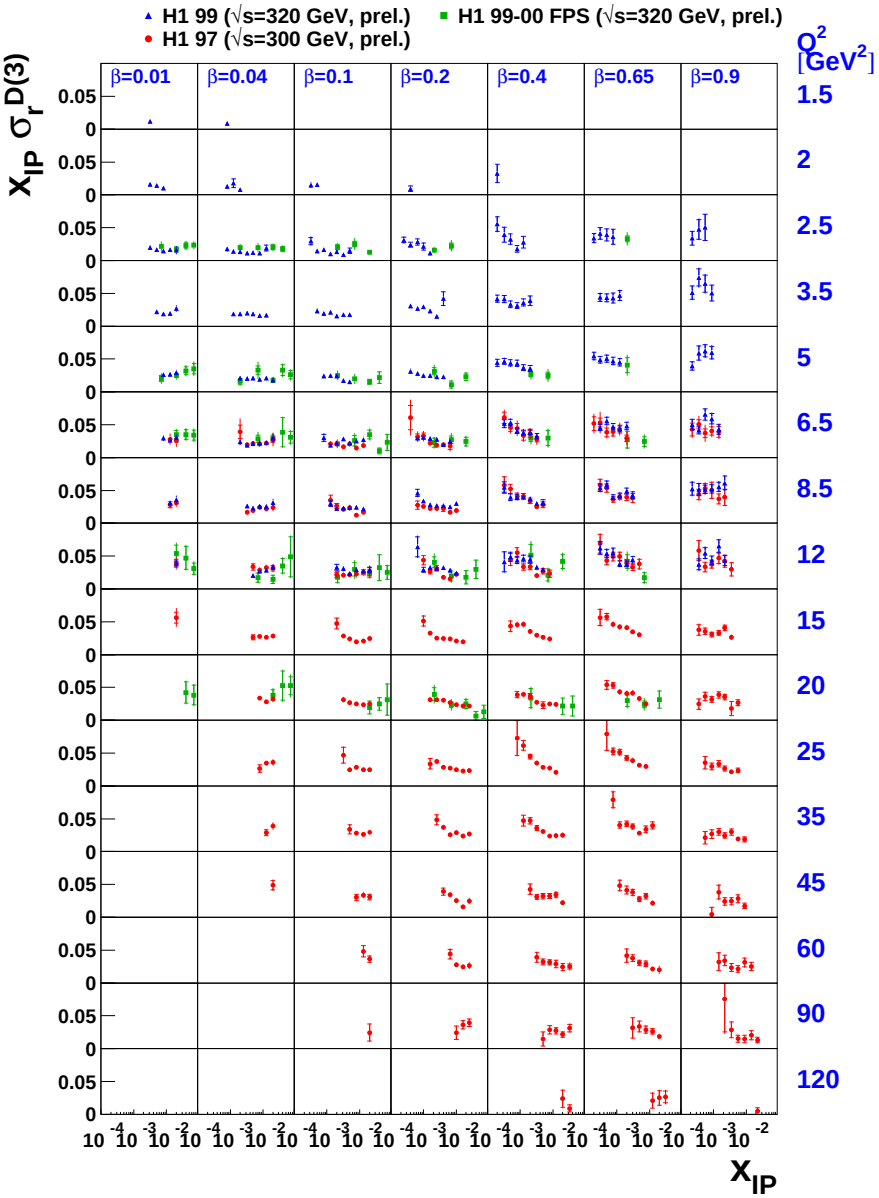

Figure 2. The diffractive reduced cross section as measured in three different samples and with different techniques is shown as a function of $x_{I\!P}$ in bins of β and Q^2.

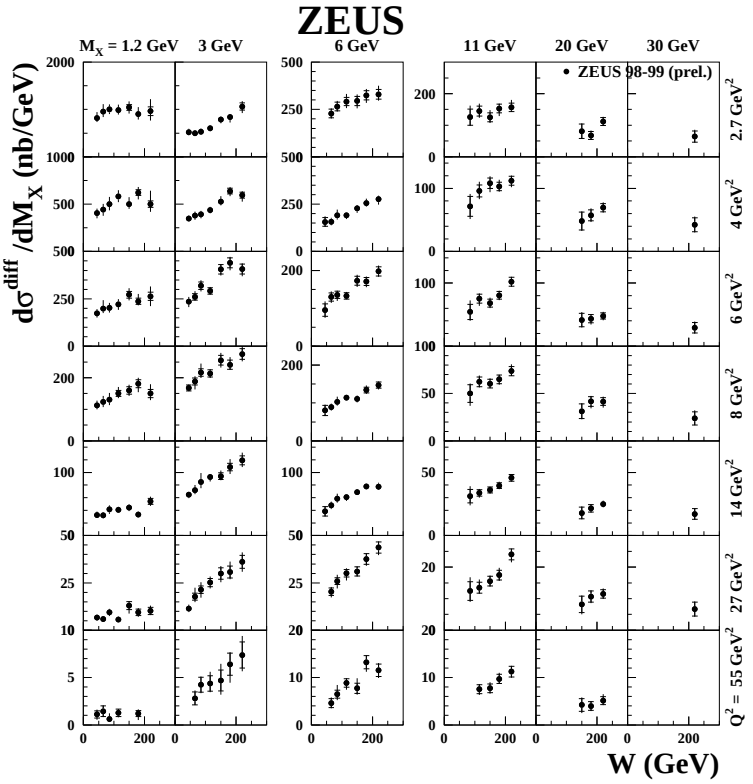

Figure 3. The differential cross section $d\sigma^{\rm diff}_{\gamma^* p\to XN}/dM_X$, $M_N < 2.3$ GeV, as a function of W in bins of M_X and Q^2.

3. General Properties of the Inclusive Diffraction at HERA

To compare the dynamics of diffractive DIS with those of inclusive DIS the ratio of the diffractive to the total inclusive cross sections is studied as a function of energy and Q^2. Fig. 5 represents just two of several such measurements. The ratio is observed to be remarkably flat both in Q^2 and in W everywhere except extreme region of high β (low M_X). The latter can be readily explained by simple kinematics (suppressing available phase space for gluon radiation close to the kinematic limit), or by the onset of higher twist effects. It is fair to note, that such behaviour is naturally expected in the models of the 2-nd class (see Sec. 1.2), in which rapidity gap formation is due to purely probabilistic mechanisms.

Approximately flat ratio as a function of W implies the same energy

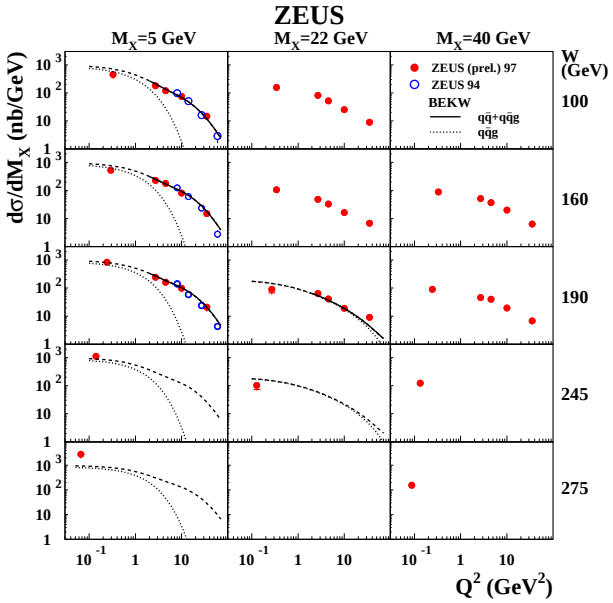

Figure 4. Q^2 dependence of the diffractive cross section $d\sigma^D_{\gamma^* p}/dM_X$ at different values of W and M_X.The solid (dashed) lines represent results of the specific dipole model fit[16] (and its extrapolation). The $q\bar{q}g$ contribution is shown by the dotted curves.

dependence for diffractive and inclusive $\gamma^* p$ cross section, which is not expected neither in Regge picture, nor in a simple two-gluon exchange QCD models for diffractive DIS.

To quantify the difference between energy dependence of σ^D and σ^{tot} one can compare the values of the Pomeron intercept, $\alpha_{I\!P}(0)$, extracted using Regge motivated fits from diffractive and inclusive DIS data. In the inclusive case [17], proton structure function can be parameterised at low $x < 0.01$ in form of $F_2(x, Q^2) = cx^{-\lambda(Q^2)}$ with $\lambda = \alpha_{I\!P}(0) - 1$. In diffractive DIS $\alpha_{I\!P}(0)$ can be obtained, after correcting for the finite values of t, from W-, or equivalently from $x_{I\!P}$-dependence of the diffractive cross section.

The results are summarized in Fig. 6. $\alpha_{I\!P}(0)$ is observed to rise with Q^2, although the error bars are still large in case of diffraction. In contrast to photoproduction where the same universal 'soft' Pomeron trajectory describes both inclusive and diffractive data, in DIS regime the Pomeron intercept extracted in diffraction is approximately half of that obtained in inclusive data. This is consistent with the above conclusion, that the energy

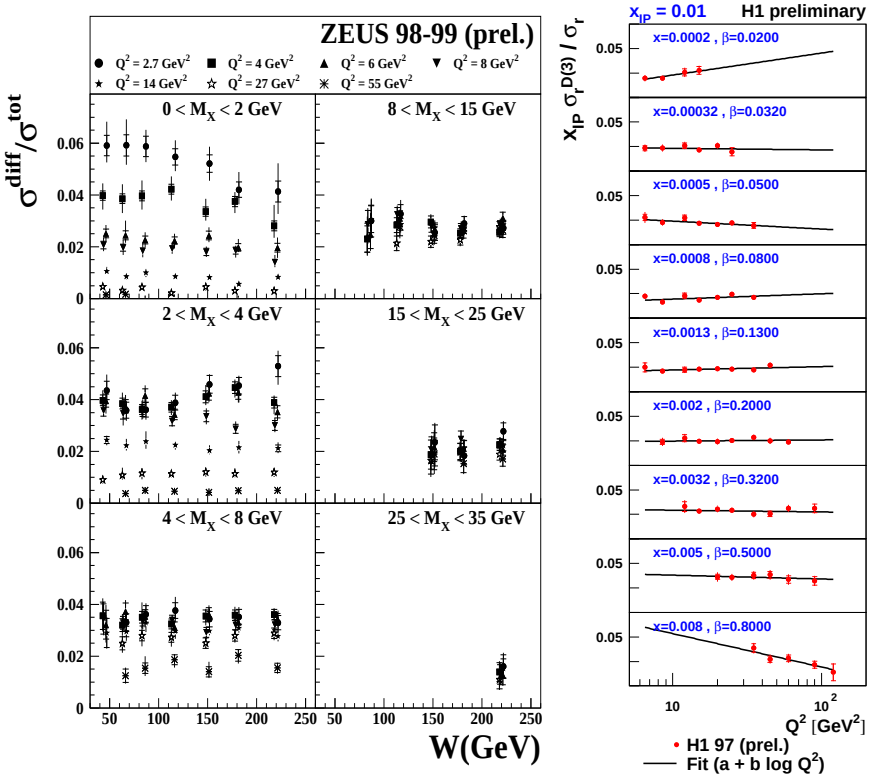

Figure 5. Ratio of diffractive to inclusive DIS cross sections as a function of W (left) and Q^2 (right).

dependence is very similar in diffractive and inclusive DIS. This surprising result is not so easy to explain, unless some sort of unitarity corrections are assumed to play a significant rôle in diffraction at HERA. Alternatively, it could point to the possibility that different proportion of soft and hard physics contributes to diffractive processes as compared to fully inclusive case, suggesting that Q^2 is not completely equivalent, or the only relevant scale in those two cases.

4. NLO QCD Fit to H1 Data and Diffractive PDFs

H1 has performed[18] a new NLO DGLAP QCD fit to the medium Q^2 data sample[11] from which diffractive parton densities are obtained. To simplify the fit Regge factorization (3) was assumed, implying that the shape of

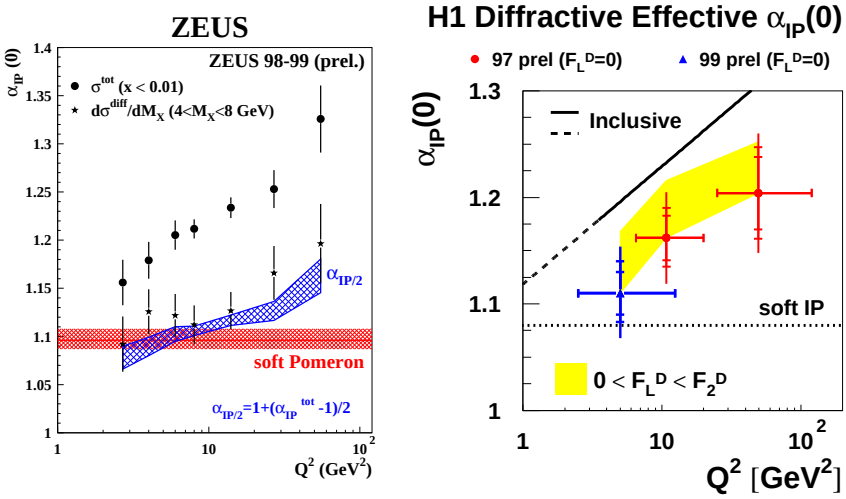

Figure 6. The intercept of the Pomeron trajectory, $\alpha_{I\!P}(0)$, as a function of Q^2 in diffractive and inclusive DIS, as determined by ZEUZ(left) and H1 (right). The cross hatched band represents 'half' of the W-rise of the total $\gamma^* p$ cross section, $\alpha_{I\!P/2} = 1 + (\alpha^{\rm tot}_{I\!P}(0) - 1)/2$.

pdf's is independent on $x_{I\!P}$. At present level of precision this assumption is justified by the data, as can be seen in Fig. 7, in which β and Q^2 dependencies are compared to the fit results.[a] Large scaling violation observed up to high values of β suggests that the diffractive exchange is dominated by gluons.

Both $I\!P$ and $I\!R$ contributions are included in the fit. The Pomeron structure is parameterised by a light flavour singlet, Σ, and a gluon, g, distributions, while for the reggeon term *pion* pdf[19] is used. The latter choice does not significantly influence the results, as the sub-leading contribution is negligible at $x_{I\!P} < 0.01$. Diffractive parton densities (*dpdf's*) are parameterised at a starting scale $Q_0^2 = 3$ GeV^2 and evolved to higher Q^2 using NLO DGLAP equations. 313 data points from the region $Q^2 > 6.5$ GeV^2 and $M_X > 2$ GeV are used to constrain 7 free parameters (3 for each the singlet and gluon distributions plus normalization of sub-leading exchange at high $x_{I\!P}$). It should be emphasized, that for the first time in diffraction

[a]Note that it is not in contradiction with the result shown in Fig. 6, as only limited Q^2 range was used in the fit. If however one would like to extend this procedure to lower Q^2, it might be necessary to drop the assumption of Regge factorization.

the experimental and model uncertainties are fully propagated to obtain error bands for resulting dpdf's.

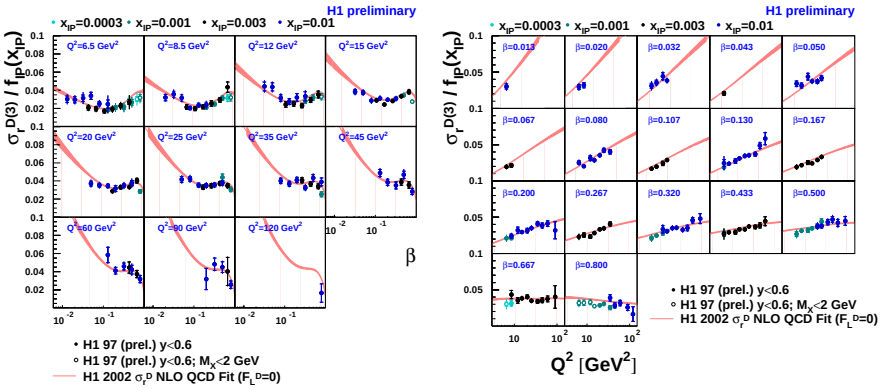

Figure 7. β (left) and Q^2 (right) dependence of the reduced cross section scaled at each $x_{I\!P}$ by the values assumed for t-integrated Pomeron flux in the QCD fits.

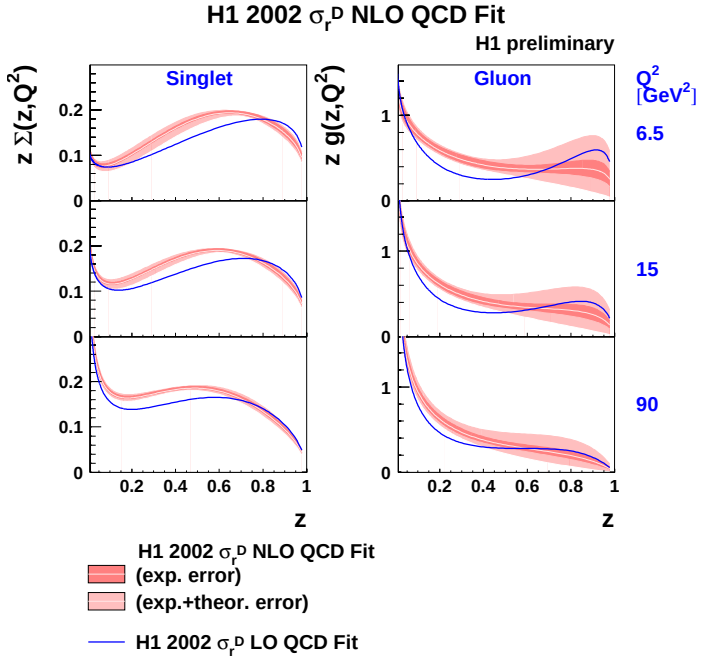

Figure 8. Diffractive parton densities obtained from the QCD fits and normalized such, that the 'Pomeron flux' is unity at $x_{I\!P} = 0.003$.

The result of the fit is shown in Fig. 8. Whereas the singlet part is well constrained, there is a substantial uncertainty in the gluon distribution at large fractional momenta z (or β), mainly due to model assumptions. The diffractive pdf's remain large up to large z and are dominated by gluons. In total $75 \pm 15\%$ of the exchange momentum is carried by gluons. Fig. 9 presents β and Q^2 dependencies of the reduced diffractive cross section at two selected values of $x_{I\!P}$. Even extrapolated beyond the region used in the fit, new pdf's give very good description of new H1 data[20] at high Q^2. One can also see, that at high $x_{I\!P}$ reggeon contribution becomes important. It is worth mentioning that new precise low Q^2 data[10] have large potential to further constrain dpdf's.

Another possible tests involve comparisons with diffractive final states[21] at HERA and TEVATRON.

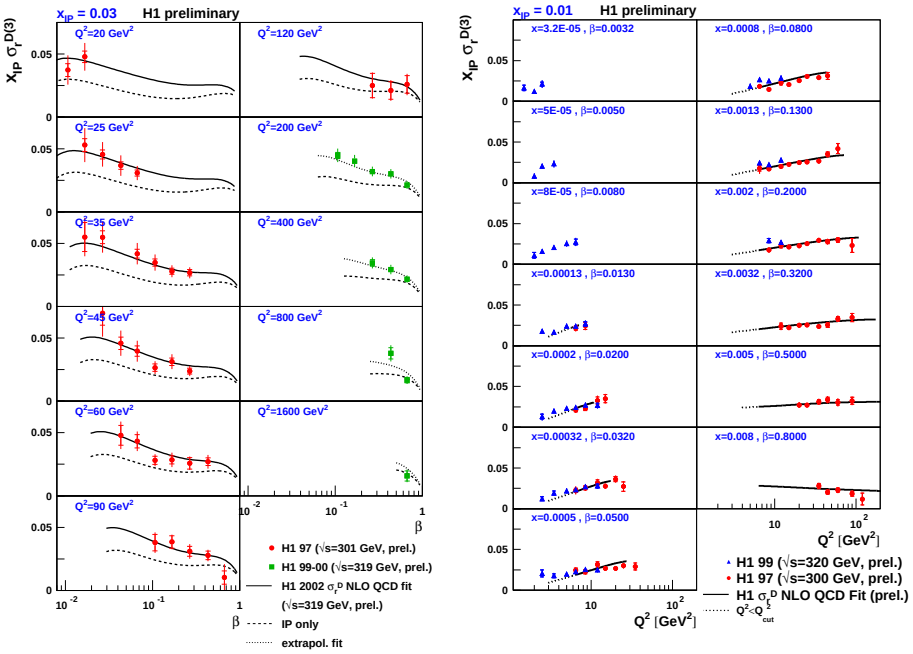

Figure 9. Reduced diffractive cross section at fixed $x_{I\!P}$ as a function of β in bins of Q^2(left) and as a function of Q^2 in bins of β (right). Also shown is the prediction for $x_{I\!P}\sigma_r^{D(3)}$ at $\sqrt{s} = 319$ GeV from the NLO QCD fit performed to the medium Q^2 data.

5. Summary

New precision measurements of inclusive diffractive DIS are now available from HERA. These data are extremely valuable to further constrain QCD motivated phenomenological models and to distinguish between different approaches to diffractive phenomena in DIS regime. New generation of diffractive parton distributions together with their uncertainties are determined from H1 data in NLO QCD framework. They can be used to test factorization properties of diffraction in different reactions. Energy dependence of the diffractive cross section has no simple explanation at the moment. It may indicate the onset of unitarity corrections (or saturation effect) is already seen in diffraction at HERA. Alternatively, it could be a manifestation of a complicated interplay between soft and hard phenomena in diffractive DIS. In spite of the recent progress a complete understanding of the nature of colour singlet exchange remains a major challenge in QCD.

References

1. T. Regge, *Nuovo Cimento* **14**, 951 (1959); *ibid.*, **18**, 947 (1960); G. Chew and S. Frautchi, *Phys. Rev. Lett.*, **7**, 394 (1961); G. Chew, S. Frautchi and S. Mandelstam, *Phys. Rev.*, **126**, 1202 (1962).
2. V.N. Gribov, *Sov. Phys. JETP*, **26**, 414 (1968).
3. G. Ingelman and P. Schlein, *Phys. Lett.*, **B152**, 256, (1985).
4. A. Edin, G. Ingelman and J. Rathsman, *Phys. Lett.*, **B366**, 371 (1996); A. Edin, G. Ingelman and J. Rathsman, *Z. Phys.*, **C 75**, 57 (1997); J. Rathsman, *Phys. Lett.*, **B452**, 364 (1999).
5. N.N. Nikolaev and B.G. Zakharov, *Z. Phys.*, **C 49**, 607 (1991); *ibid.*, **C 53**, 331 (1992); A.H. Mueller, *Nucl. Phys.*, **B 415**, 373 (1994).
6. W. Buchmüller, T. Gehrmann and A. Hebecker, *Nucl. Phys.*, **B 537**, 477 (1999); K. Golec-Biernat and M. Wüsthoff, *Phys. Rev.*,**D 59**, 014017 (1999); J. Bartels, K. Golec-Biernat and H. Kowalski, *Phys. Rev.*,**D 66**, 014001 (2002).
7. J. Collins, *Phys. Rev.*, **D 57**, 3051 (1998); err. - *ibid.* **D 61**, 019902 (2000).
8. ZEUS Coll., A. Bamberger *et al.*, *Nucl. Inst. Meth.*, **A450**, 235 (2000).
9. ZEUS Coll., M. Derrick *et al.*, *Z. Phys.* **C 70**, 391 (1966);
   H1 Coll., C. Adloff *et al.*, *Z. Phys.* **C 76**, 613 (1997).
10. H1 Coll., paper 88 subm. to EPS 2003.
11. H1 Coll., paper 808 subm. to EPS 2001.
12. H1 Coll., paper 984 subm. to ICHEP 2002.
13. ZEUS Coll., paper 821 subm. to ICHEP 2002; paper 538 subm. to EPS 2003.
14. ZEUS Coll., paper 566 subm. to EPS 2001; paper 540 subm. to EPS 2003.
15. ZEUS Coll., J. Breitweg *et al.*, *Phys. Lett.*, **B487**, 53 (2000).
16. J. Bartels *et al.*, *Eur.Phys. J.*, **C7**, 443 (1999).
17. H1 Coll., C. Adloff *et al.*, *Phys. Lett.*, **B520** 183 (2001).
18. H1 Coll., paper 89 subm. to EPS 2003.

19. J. Owens, *Phys. Rev.*, **D 30**, 913 (1984)
20. H1 Coll., paper 90 subm. to EPS 2003.
21. N. Vlasov, these proceedings.